ORIGINAL ARTICLE

Effects of atorvastatin on autophagy in skeletal muscles of diabetic rats

Bingquan Yang, Jie Sun, Yang Yuan, Zilin Sun* (iD)

Department of Endocrinology, Zhongda Hospital, Institute of Diabetes, School of Medicine, Southeast University, Nanjing, Jiangsu, China

ABSTRACT

Aims/Introduction: Atorvastatin is usually used to decrease the amount of fatty substances in individuals with type 2 diabetes mellitus. However, it can cause side-effects, such as breakdown of skeletal muscle tissue. The present study focused on the effects of atorvastatin on autophagy of the skeletal muscles in diabetic rats.

Materials and Methods: Diabetes in rats in the diabetic (D) and atorvastatin (T) groups was induced using streptozotocin (65 mg/kg, intraperitoneal injection). Next, rats in the T group were treated with atorvastatin (10 mg/kg/day, intragastric administration), whereas rats in the control and D groups were given water. Additionally, the rats in T and D groups were fed a high-fat and high-sugar diet for 10 weeks. Subsequently, the histopathological changes, and expression levels of microtubule-associated protein 1 light chain 3 (LC3)-I/-II and p62 in the skeletal muscle specimens in the three groups were analyzed.

Results: Rats in the T group had reduced lipid droplets, cholesterol and low-density lipoprotein ($P < 0.05$) levels than those in the D group. Disordered atrophic myocytes, incrassated vascular walls and decreased cross-sectional area of type I fibers were found using hematoxylin–eosin and adenosine triphosphatase staining in the D and T groups. The messenger ribonucleic acid and protein levels of LC3-II and the LC3-II/LC3-I ratio were increased in the T group compared with those in the other groups ($P < 0.05$), whereas the protein level of p62 showed the opposite trend.

Conclusions: Atorvastatin enhanced the autophagy level of skeletal muscles to decrease lipid deposition, which possibly exacerbated myopathy.

INTRODUCTION

Diabetes has become a major threat to human health globally. In China, the overall incidence of diabetes is approximately 9.7%, particularly in those aged >60 years, in whom the incidence rate is >20%[1]. Previous studies found that the incidence of skeletal muscle disease, which is independently associated with diabetes mellitus, in diabetes patients is double than in healthy individuals[2,3].

Recently, abnormal autophagy has been confirmed to be an important factor in the induction of skeletal muscle injury. A report suggested that excessive accumulation of autophagosomes in skeletal muscle leads to autophagy-associated myopathy syndrome[4]. Elucidation of the mechanism underlying autophagy in diabetic skeletal muscle might be very important for the prevention and treatment of diabetic myopathy.

The autophagy-related microtubule-associated protein 1 light chain 3 (LC3) is commonly used for the quantification of autophagic activity. The cytosolic form of LC3-I is immediately yielded after the cleavage of LC3 at the carboxy terminus. During autophagy, it is conjugated to a phospholipid to form endogenous LC3-II[5], and the LC3-II/LC3-I ratio increases[6]. Therefore, the LC3-II/LC3-I ratio is often used to determine the activation of autophagy[7]. In addition, p62 facilitates the degradation of ubiquitinated protein aggregates by autophagy[8]. It is a selective substrate for autophagy and directly interacts with LC3 to mediate the degradation of ubiquitinated protein aggregates by autophagy[9].

Atorvastatin is not only used to decrease the amount of fatty substances, such as cholesterol and triglycerides, but also to lower the risk of vascular complications in individuals with type 2 diabetes mellitus[10,11]. However, it can cause potentially serious side-effects, including the breakdown of skeletal muscle tissue[12]. Whether atorvastatin is associated with the level of autophagy and how atorvastatin affects skeletal muscle autophagy in diabetes patients remain unclear. In the present study,

the autophagy and lipid deposition levels before and after treatment with atorvastatin in different types of skeletal muscle in diabetic rats were determined. The results might help to further investigate the effects of atorvastatin in skeletal muscle and atorvastatin-induced autophagy in diabetic rats.

METHODS

Animals
Six-week-old male Sprague–Dawley rats (weight 200.15 ± 20.46 g) purchased from Shanghai SLAC Laboratory Animal Co., Ltd. (Shanghai, China), were pre-housed in a specific pathogen-free environment and maintained at the Animal Experiment Center of Southeast University. This study was approved by the institutional review board of Southeast University. The rats were kept in cages (3–4 rats per cage), and were permitted free access to both feed and water.

Groups and treatment
After 7 days of pre-adaptation, the rats were randomly divided into three groups: the control group (C; six rats), the diabetic model group (D; six rats) and the atorvastatin group (T; six rats). To establish a rat model of streptozotocin (STZ)-induced diabetes, the rats of the latter two groups were injected intraperitoneally with STZ (65 mg/kg; Sigma, St. Louis, MO, USA), which was dissolved in 0.1 mmol/L citric acid buffer. Rats in the C group were injected intraperitoneally with equal doses of citrate buffer. The oral glucose tolerance test was carried out to verify the diabetes model. Next, rats in the T group were treated with atorvastatin (10 mg/kg/day, dissolved in distilled water; Sigma) by gavage, while the other groups were given the same amount of water. The rats of the D and T groups were fed with a high-fat and high-sugar diet for 10 weeks.

Sampling
The rats were anesthetized intraperitoneally with 2% thiopental sodium (50 mg/kg; Zhejiang Otsuka Pharmaceutical Co., Ltd., Zhejiang, China). The extensor digitorum longus (EDL), soleus and plantaris were removed from the hind limb of the rat on ice. Some fresh tissues were snap-frozen in isopentane, embedded by optimal cutting temperature compound, quick frozen in liquid nitrogen and sliced on a cryostat microtome (CM 1850; Leica Instruments, Wetzlar, Germany).

Hematoxylin–eosin staining, oil red O staining and adenosine triphosphatase staining on frozen sections
Hematoxylin–eosin (HE) staining was carried out using HE staining kits (KGA224; Nanjing KeyGen Biotech Co., Ltd., Nanjing, China), in accordance with the manufacturer's instructions. Neutral lipid-fixed stromal-vascular cells were subjected to conventional histochemical staining with oil red O and hematoxylin[13]. Histochemical adenosine triphosphatase staining was carried out as previously described[14]. Images of the stained sections were obtained under a microscope (BX52; Olympus, Tokyo, Japan). The acquired signals of different types of muscle fibers were analyzed using Simple PCI software (Meyer Instruments, Inc., Houston, TX, USA), and the physiological cross-sectional area of each muscle and the percentage of total muscle area were determined.

Real-time polymerase chain reaction analysis of the expression level of LC3-II
Total ribonucleic acid (RNA) was extracted from the skeletal muscle samples stored at −80°C using TRIzol (Invitrogen, Carlsbad, CA, USA). Denaturing formaldehyde agarose gel electrophoresis was carried out to determine RNA integrity, and a GeneQuant spectrophotometer (Pharmacia, Piscataway, NJ, USA) was used to measure the concentration and purity of the RNA. Reverse transcription was carried out following the instructions of the RevertAid First Strand cDNA Synthesis Kit (Fermentas, Waltham, MA, USA). The messenger RNA (mRNA) level of LC3-II was determined by real-time polymerase chain reaction analysis using IQ SYBR Green Supermix (Bio-Rad, Hercules, CA, USA). β-Actin was used as an internal control. The primers of LC3-II were forward primer, 5′-GATGTCCGACTTATTCGAGAGC-3′ and reverse primer, 5′-TTGAGCTGTAAGCGCCTTCTA-3′. The primers of glyceraldehyde 3-phosphate dehydrogenase were forward primer, 5′-CACCCATGACGAACATGGG-3′ and reverse primer, 5′-TTCCAGGAGCGAGATCCCT-3′ (reverse).

Western blotting assay in skeletal muscle samples
The skeletal muscle samples stored at −80°C were homogenized; the supernatant was collected using total protein extraction kits (Nanjing KeyGen Biotech Co., Ltd.). The total protein content of the pooled supernatants was measured using the bicinchoninic acid method (Nanjing KeyGen Biotech Co., Ltd.). The protein levels of LC3-II and p62 were determined using anti-LC3-I (1:1000), anti-LC3-II (1:1000) and anti-p62 (1:800) antibodies (Sigma). The secondary antibody was horseradish peroxidase-labeled antibody (1:5000), and glyceraldehyde 3-phosphate dehydrogenase was used as a control.

Statistical analysis
All of the data were tested for a normal distribution. When the criteria for a normal distribution were not met, the data were converted to a normally distributed form through logarithmic transformation. The obtained data are expressed as mean ± standard deviation. Differences between groups were analyzed using one-way ANOVA followed by post-hoc analysis using the Student–Newman–Keuls test. Data analysis was carried out using SPSS18.0 (SPSS Inc., Chicago, IL, USA). A *P*-value of <0.05 was considered statistically significant.

RESULTS

Bodyweight, blood lipid and blood glucose of Sprague–Dawley rats in the three groups
The bodyweight of the rats in the D group was significantly lower than that in the C group (D: 303.00 ± 18.57 g, C:

460.40 ± 21.41 g; $P < 0.05$). There was no significant difference in the bodyweight between the rats in the T and D groups ($P > 0.05$; Table 1).

The blood glucose level in the rats in the D group was significantly higher than that in the C group (D: 25.52 ± 2.87 mmol/L, C: 6.40 ± 0.61 mmol/L; $P < 0.05$); however, there was no significant difference in this regard between the rats in the T and D groups (T: 23.48 ± 5.97 mmol/L, D: 25.52 ± 2.87 mmol/L; $P > 0.05$; Table 1).

The levels of triglyceride, cholesterol and low-density lipoprotein in the rats in the D group were significantly higher than that in the C group (all $P < 0.05$). In addition, the cholesterol and low-density lipoprotein levels in the rats in the T group were lower than those of the rats in the D group (all

Table 1 | Biochemical parameters of rats in different groups

	Control	Diabetes	Atorvastatin treated
Weight (g)	460.40 ± 21.41	303.00 ± 18.57*	296.00 ± 49.66
Blood glucose (mmol/L)	6.40 ± 0.61	25.52 ± 2.87*	23.48 ± 5.97
Triglyceride (mmol/L)	0.38 ± 0.09	1.89 ± 0.25*	1.08 ± 0.88
Cholesterol (mmol/L)	1.70 ± 0.24	11.60 ± 3.98*	4.43 ± 2.35**
Low-density lipoprotein (mmol/L)	0.76 ± 0.07	4.72 ± 0.90*	1.87 ± 0.73**

Data presented as mean ± standard deviation. *$P < 0.05$ compared with the control group; **$P < 0.05$ compared with the diabetic group
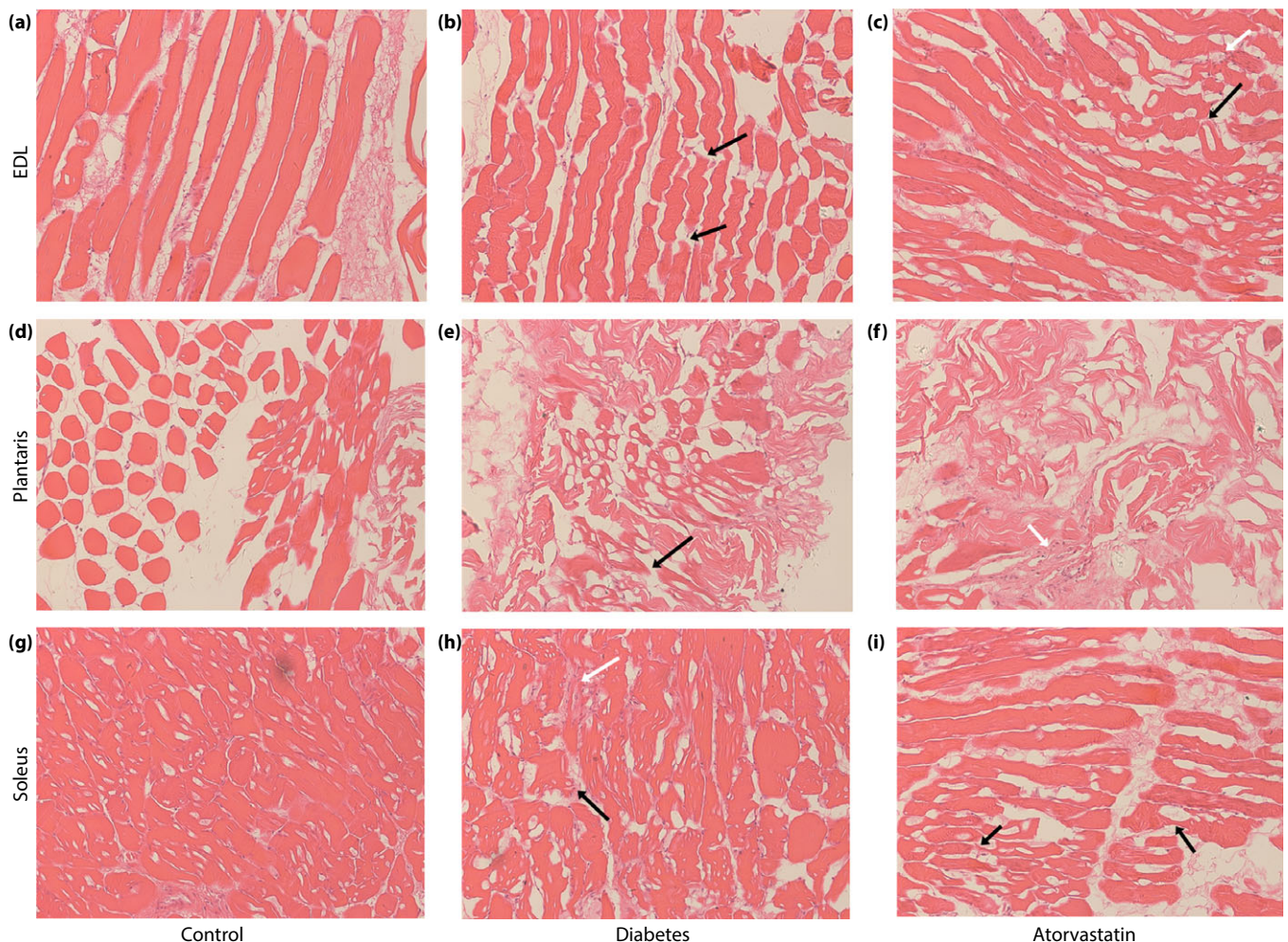

Figure 1 | Hematoxylin–eosin staining images of the extensor digitorum longus (EDL), plantaris and soleus in control, diabetes and atorvastatin groups. (a–c) EDL. (d–f) Plantaris. (g–i) Soleus. Muscle fiber atrophy and disruption (black arrow) or centralized nuclei (white arrow) were observed in the EDL, plantaris and soleus of the diabetes and atorvastatin groups (original magnification: ×200).

$P < 0.05$); however, the triglyceride level in the rats of the T group showed no significant difference ($P > 0.05$; Table 1).

Morphological changes of skeletal muscle

The HE staining showed that, compared with the rats in the C group, disordered arrangement of cells, interstitial edema, cytoplasmic autolysis, actin filament disruption, muscle fiber atrophy, muscle cell hyperplasia and inflammatory cell infiltration were observed in the EDL (Figure 1a), plantaris (Figure 1b) and soleus (Figure 1c) of the rats in the D group. No significant differences in these variables were found between the rats in the T and D groups.

The oil red O staining showed that there were a large number of lipid droplets in the rats in the D group, a small amount of lipid droplets in the rats in the T group and especially in that of the C group (Figure 2).

The cross-sectional areas of type 1 fibers in the EDL, plantaris and soleus muscles of the rats in the D group were significantly lower than those of the rats in the C group (all $P < 0.001$). No significant differences were found between the EDL, plantaris and soleus muscles of the rats in the T and D groups ($P = 0.139$, $P = 0.258$ and $P = 0.241$, respectively; Figure 3).

mRNA levels of LC3-II and LC3-I in the three groups

The mRNA levels of LC3-II in the EDL, plantaris and soleus muscles in the rats in the D group were significantly higher than those in the rats in the C group ($P = 0.012$, $P = 0.011$ and $P = 0.019$, respectively; Figure 4). The mRNA levels of LC3-II in the plantaris and soleus muscles in the rats in the T group were higher than those in the D group ($P = 0.039$ and $P = 0.002$, respectively; Figure 4).

LC3-II/LC3-I ratio in the three groups

The LC3-II/LC3-I ratios in the EDL, plantaris and soleus muscles of the rats in the D group were higher than those of the rats in the C group ($P = 0.013$, $P = 0.009$ and $P = 0.027$,
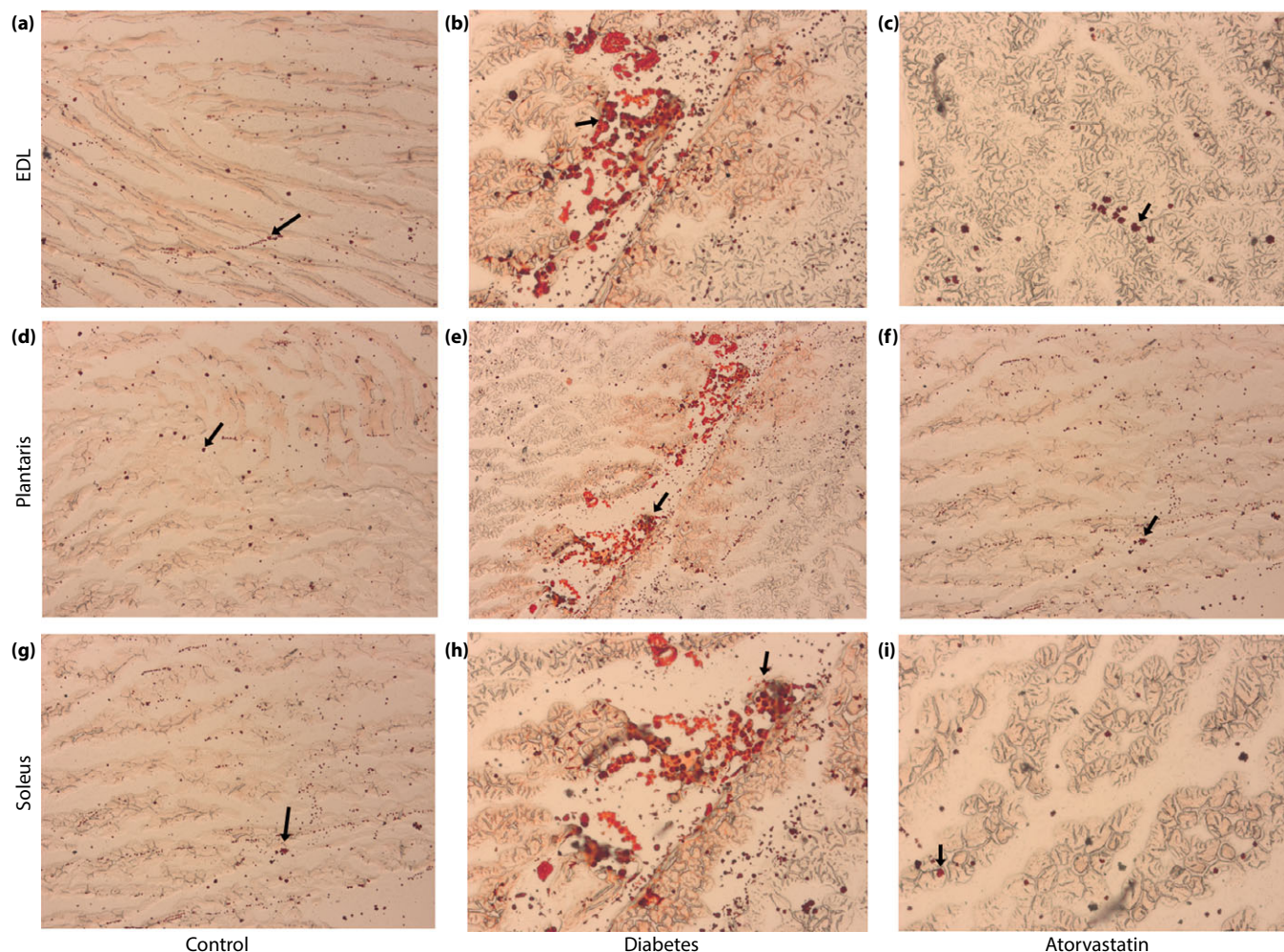

Figure 2 | Oil red O staining images of (a–c) the extensor digitorum longus, (d–f) plantaris and (g–i) soleus in the three groups. The lipid droplets (black arrow) in the rats of the three groups were found (original magnification: ×200).
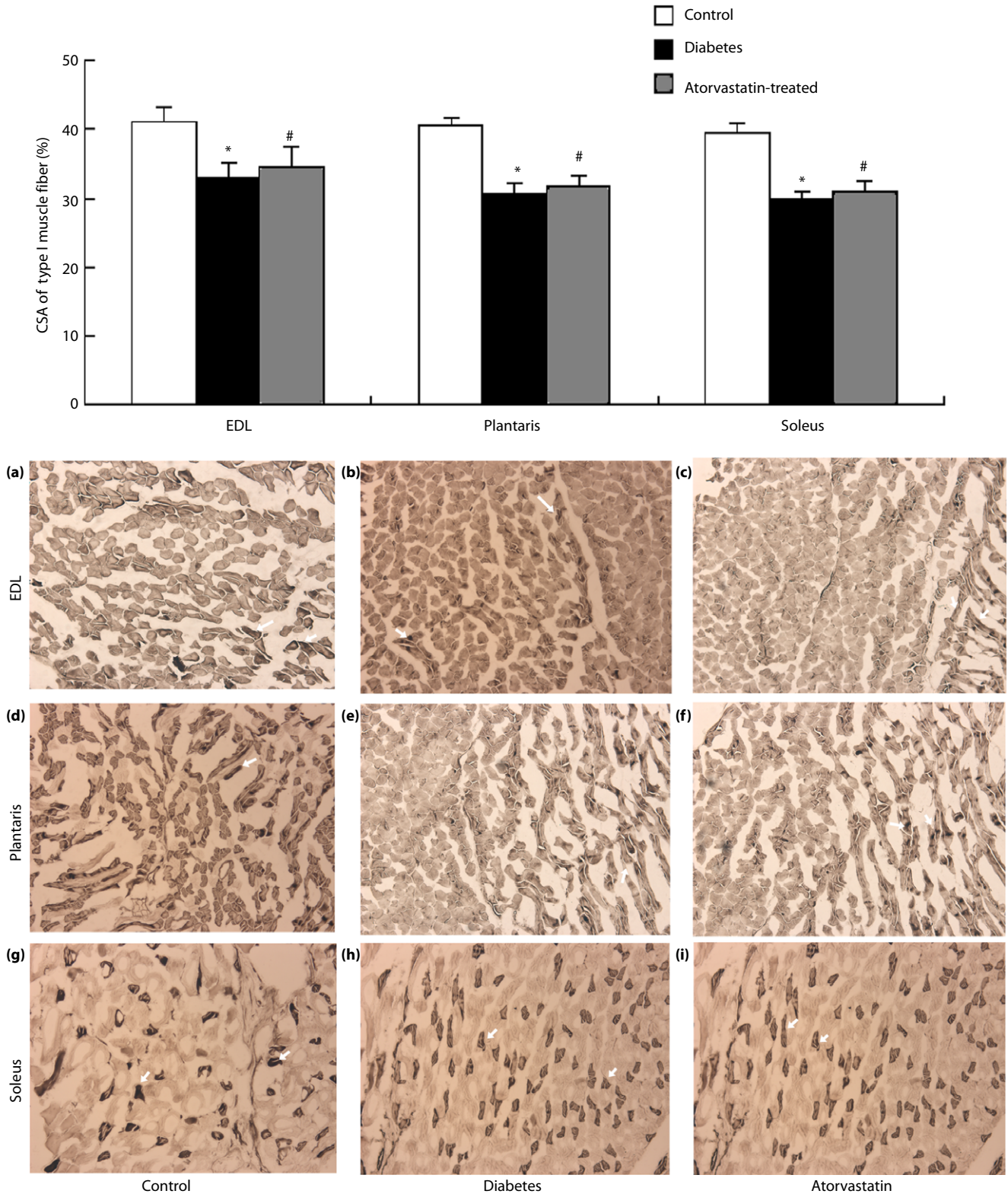
Figure 3 | The cross-sectional area (CSA) of type I muscle fibers (upper) and the adenosine triphosphatase staining of different skeletal muscles in rats (lower). Type I muscle fibers (white arrow) were stained in all the skeletal muscles of rats in the three groups (original magnification: ×200). *$P < 0.05$ indicates that there are significant differences when compared with the control group; #$P > 0.05$ indicates that there are significant differences when compared with the diabetic group. (a–c) Extensor digitorum longus (EDL). (d–f) Plantaris. (g–i) Soleus.
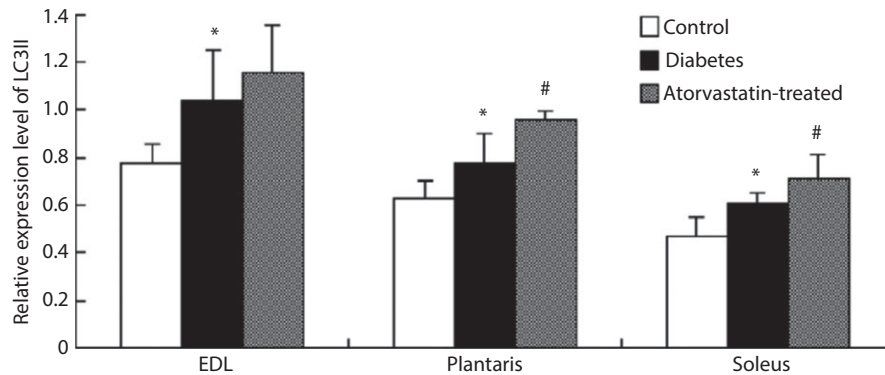
Figure 4 | Relative expression of microtubule-associated protein 1 light chain 3 (LC3)-II messenger ribonucleic acid in different skeletal muscles in rats. *$P < 0.05$ indicates that there are significant differences when compared with the control group; #$P < 0.05$ indicates that there are significant differences when compared with the diabetic group. EDL, extensor digitorum longus.

Figure 5 | (a) Western blotting of microtubule-associated protein 1 light chain 3 (LC3)-I/LC3-II and (b) the LC3-II/LC3-I ratio in different skeletal muscles in rats. *$P < 0.05$ indicates that there are significant differences when compared with the control group; #$P < 0.05$ indicates that there are significant differences when compared with the diabetic group. EDL, extensor digitorum longus.
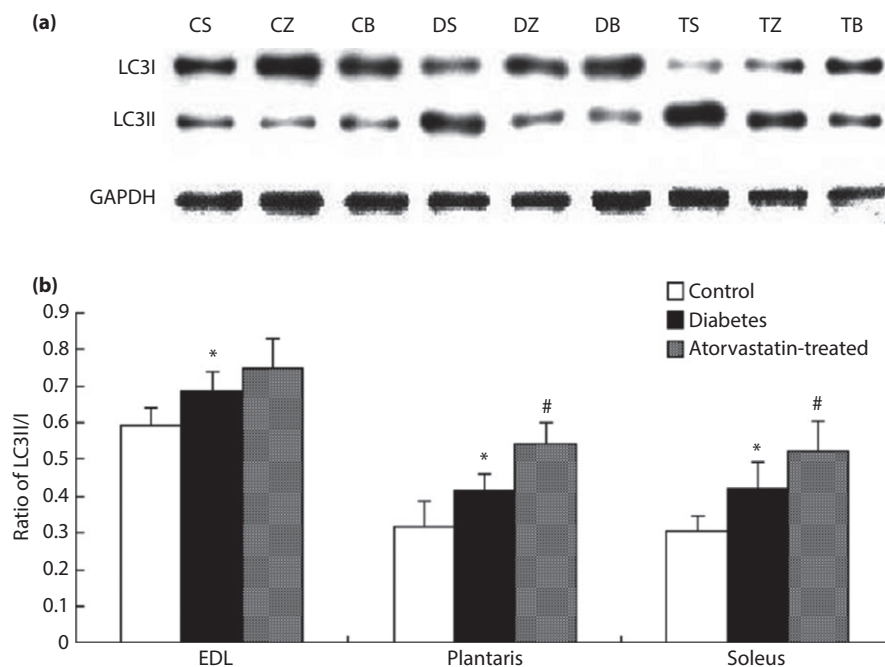
respectively). The LC3-II/LC3-I ratios in the plantaris and soleus muscles of the rats in the T group were higher than those in the D group ($P = 0.017$ and $P = 0.002$, respectively; Figure 5).

Protein level of p62 in the three groups

The protein levels of p62 in the EDL, plantaris and soleus muscles of the rats in the D group were lower than that of the rats in the C group ($P = 0.010$, $P = 0.027$ and $P = 0.034$, respectively; Figure 6), and those of the rats in the T group were the

lowest ($P = 0.049$, $P = 0.019$ and $P = 0.026$, respectively; Figure 6).

DISCUSSION

Skeletal myopathy is one of the serious complications of diabetes patients. Autophagy has been found to be involved in atrophy and myopathy in skeletal muscles[15]. In the present study, a diabetic rat model was established by the intraperitoneal injection of STZ. The change of autophagy in different skeletal muscles and the effects of atorvastatin on autophagy of
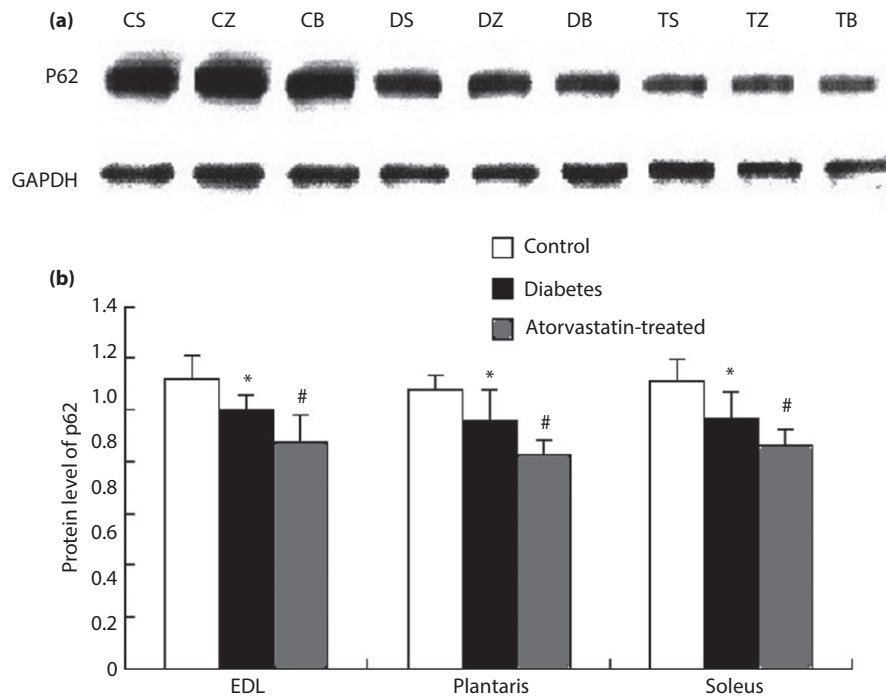
Figure 6 | Western blotting of p62 (a) and the expression of p62 in different skeletal muscles in rats (b). *$P < 0.05$ compared with the control group; #$P < 0.05$ compared with the diabetic group. EDL, extensor digitorum longus; GAPDH, glyceraldehyde 3-phosphate dehydrogenase C, the control group; D, the diabetic model group; T, the atorvastatin group.

these skeletal muscles in diabetic rats are discussed in this article.

The average blood glucose level of the rats in the D group was significantly higher than that of the rats in the C group, which indicated the successful establishment of the diabetic model. Previous studies have shown that atorvastatin can reduce triglyceride and leptin levels to improve insulin resistance[16]. A study showed that atorvastatin cannot improve insulin sensitivity; however, it could increase the risk of diabetes[17]. In addition, an animal experiment showed that insulin signaling was impaired after atorvastatin treatment, along with reduced glucose uptake in adipocytes and inhibited insulin secretion in islet cells[18]. In the present study, the blood glucose of the rats in the D group was not changed after atorvastatin treatment. This might be because atorvastatin dose-dependently inhibited the secretion of insulin. A high dose of atorvastatin can inhibit the secretion of insulin, while at the same time, atorvastatin can increase the sensitivity to insulin, with the two effects essentially offsetting each other.

The HE staining results suggested that varying degrees of muscle atrophy were shown in different muscle fiber types. Because soleus and EDL mainly comprise type I[19] and type II fibers[20], respectively, whereas plantaris comprises both type 1 and type 2 fibers[21], the results suggested that the conversion of type II to type I fibers was found in diabetic rats, and the atorvastatin treatment could not counteract these changes. In addition, the alteration of glycolytic muscle fibers into oxidative

muscle fibers was also found in diabetic rats, which was also not changed after atorvastatin treatment. Furthermore, skeletal muscle structure abnormalities were found in both the T and D groups. In addition, the oil red O staining assay showed that atorvastatin treatment reduced skeletal muscle lipid deposition in diabetic rats, which is consistent with previous research[22]. Furthermore, atorvastatin as a 3-hydroxy-3-methyl-glutaryl-coenzyme A reductase inhibitor can prevent the development of cardiovascular and atherosclerotic diseases. In a previous study, statin-induced myopathy was shown to be due to the blockade of cholesterol synthesis dependent on the deficiencies of 3-hydroxy-3-methyl-glutaryl-coenzyme A reductase enzyme activity in the skeletal muscle[23]. Therefore, atorvastatin can reduce lipid levels and affect lipid metabolism, but has little effect on glucose metabolism and muscle cell injury.

The reverse transcription polymerase chain reaction and western blotting assay showed significant differences among the three groups in the expression levels of LC3-II, LC3-I and p62. This suggested that the autophagy level is tightly associated with blood glucose concentration and atorvastatin treatment. A previous study proved that diabetes induced by STZ increases skeletal muscle autophagy activity, which is consistent with the results of the present study[24]. Therefore, the increase of the autophagy level might be due to the increased lipid deposition in skeletal muscle activating the autophagolysosome system. In addition, inflammatory cell infiltration, enhanced inflammatory response and oxidative stress in the skeletal muscle induce the

increased production of reactive oxygen species, thereby resulting in an increase in autophagy levels. The activation of autophagy can be a protective mechanism to maintain the balance of glycolipid metabolism, thereby reducing the risk of damage to the body. Atorvastatin protects vascular smooth muscle cells from calcification by the induction of autophagy in cardiovascular remodeling[25]. The present study shows that atorvastatin can enhance the autophagy level of skeletal muscles through lipid deposition and inflammatory response.

Several limitations in the present study should be emphasized. In this study, neither normal rats treated with atorvastatin were used as controls, nor were they used in a different time-course of diabetes. In addition, the dose of atorvastatin was not set at different concentrations, and it was unclear whether different doses of atorvastatin caused different levels of autophagy in skeletal muscle. Furthermore, additional factors involved in the autophagy-related pathway should be determined to clarify the precise signaling mechanism mediating autophagy.

In conclusion, the present study showed that blood glucose and triglyceride levels were not significantly impacted by atorvastatin. In addition, the drug did not affect muscle glucose metabolism, and can enhance the autophagy level of different skeletal muscles, possibly through increased lipid deposition, enhanced inflammatory response and oxidative stress. In other words, the activation of autophagy possibly exacerbated atrorvastatin-induced myopathy.

ACKNOWLEDGMENTS

DISCLOSURE

The authors declare no conflict of interest.

REFERENCES

1. Yang WY, Lu JM, Weng JP, *et al.* Prevalence of diabetes among men and women in China. *N Engl J Med* 2010; 362: 2425–2426; author reply 2426.
2. Andreassen CS, Jakobsen J, Ringgaard S, *et al.* Accelerated atrophy of lower leg and foot muscles—a follow-up study of long-term diabetic polyneuropathy using magnetic resonance imaging (MRI). *Diabetologia* 2009; 52: 1182–1191.
3. Kim TN, Park MS, Yang SJ, *et al.* Prevalence and determinant factors of sarcopenia in patients with type 2 diabetes: the Korean Sarcopenic Obesity Study (KSOS). *Diabetes Care* 2010; 33: 1497.
4. Malicdan MC, Noguchi S, Nishino I. Monitoring autophagy in muscle diseases. *Methods Enzymol* 2009; 453: 379.
5. Mann SS, Hammarback JA. Molecular characterization of light chain 3. A microtubule binding subunit of MAP1A and MAP1B. *J Biol Chem* 1994; 269: 11492–11497.
6. Tanida I, Ueno T, Kominami E. LC3 conjugation system in mammalian autophagy. *Int J Biochem Cell Biol* 2004; 36: 2503.
7. Mizushima N, Yoshimorim T, Levine B. Methods in mammalian autophagy research. *Cell* 2010; 140: 313–326.
8. Guo X, Dong Y, Yin S, *et al.* Patulin induces pro-survival functions via autophagy inhibition and p62 accumulation. *Cell Death Dis* 2013; 4: e822.
9. Pankiv S, Clausen TH, Lamark T, *et al.* p62/SQSTM1 binds directly to Atg8/LC3 to facilitate degradation of ubiquitinated protein aggregates by autophagy. *J Biol Chem* 2007; 282: 24131.
10. Shankar RR, Zhu JS, Baron AD. Glucosamine infusion in rats mimics the β-cell dysfunction of non—insulin-dependent diabetes mellitus. *Metab Clin Exp* 1998; 47: 573–577.
11. Jones KD, Couldwell WT, Hinton DR, *et al.* Lovastatin induces growth inhibition and apoptosis in human malignant glioma cells. *Biochem Biophys Res Comm* 1995; 205: 1681–1687.
12. Toussirot É, Michel F, Meneveau N. Rhabdomyolysis occurring under statins after intense physical activity in a marathon runner. *Case Rep Rheumatol* 2015; 2015: 1–2.
13. Xu H, Barnes GT, Yang Q, *et al.* Chronic inflammation in fat plays a crucial role in the development of obesity-related insulin resistance. *J Clin Invest* 2003; 112: 1821–1830.
14. Brooke MH, Kaiser KK. Three "myosin adenosine triphosphatase" systems: the nature of their pH lability and sulfhydryl dependence. *J Histochem Cytochem* 1970; 18: 670–672.
15. Levine B. Autophagy in the pathogenesis of disease. *Cell* 2008; 132: 27–42.
16. Lv P, Huang J, Yang J, *et al.* Autophagy in muscle of glucose-infusion hyperglycemia rats and streptozotocin-induced hyperglycemia rats via selective activation of m-TOR or FoxO3. *PLoS One* 2014; 9: e87254.
17. Raben N, Hill V, Shea L, *et al.* Suppression of autophagy in skeletal muscle uncovers the accumulation of ubiquitinated proteins and their potential role in muscle damage in Pompe disease. *Hum Mol Genet* 2008; 17: 3897–3908.
18. Fukuda T, Roberts A, Ahearn M, *et al.* Autophagy and lysosomes in Pompe disease. *Autophagy* 2006; 2: 318–320.
19. Khan M, Couturier A, Kubens JF, *et al.* Niacin supplementation induces type II to type I muscle fiber transition in skeletal muscle of sheep. *Acta Vet Scand* 2013; 55: 85.
20. Lópezgarcía K, Mariscaltovar S, Martínezgómez M, *et al.* Fiber type characterization of striated muscles related to micturition in female rabbits. *Acta Histochem* 2014; 116: 481–486.
21. Mizunoya W, Iwamoto Y, Shirouchi B, *et al.* Dietary fat influences the expression of contractile and metabolic genes in rat skeletal muscle. *PLoS One* 2013; 8: e80152.

22. Jannig PR, Moreira JBN, Bechara LRG, *et al.* Autophagy signaling in skeletal muscle of infarcted rats. *PLoS One* 2014; 9: e85820.

23. Osaki Y, Nakagawa Y, Miyahara S, *et al.* Skeletal muscle-specific HMG-CoA reductase knockout mice exhibit rhabdomyolysis: a model for statin-induced myopathy. *Biochem Biophys Res Comm* 2015; 466: 536.

24. Xia L, Lei Z, Shi Z, *et al.* Enhanced autophagy signaling in diabetic rats with ischemia-induced seizures. *Brain Res* 2016; 1643: 18–26.

25. Liu D, Cui W, Liu B, *et al.* Atorvastatin protects vascular smooth muscle cells from TGF-β1-stimulated calcification by inducing autophagy via suppression of the β-catenin pathway. *Cell Physiol Biochem* 2014; 33: 129.